The five homologous CiaR-controlled Ccn sRNAs of *Streptococcus pneumoniae* modulate Zn-resistance.

Nicholas R. De Lay[1,4#], Nidhi Verma[1], Dhriti Sinha[1], Abigail Garrett[2], Maximillian Osterberg[3], Spencer Reiling[1], Daisy Porter[1], David P. Giedroc[3], and Malcolm E. Winkler[2]

[1]Department of Microbiology and Molecular Genetics, McGovern Medical School, University of Texas Health Science Center, Houston, TX 77030, USA

[2]Department of Biology, Indiana University Bloomington, Bloomington, Indiana 47405

[3]Department of Chemistry, Indiana University, Bloomington, Bloomington, Indiana 47405

[4]MD Anderson Cancer Center UTHealth Graduate School of Biomedical Sciences, University of Texas Health Science Center, Houston, TX 77030, USA

Running Title: Loss of the Ccn sRNAs cause Zn hypersensitivity

Keywords: small RNA; post-transcriptional regulation; Zn homeostasis; Mn homeostasis; CiaRH

[#] Correspondence should be sent to Nicholas R. De Lay (Tel: +1 (713) 500-6293; Email: nicholas.r.delay@uth.tmc.edu)

ABSTRACT

Zinc is a vital transition metal for *Streptococcus pneumoniae*, but is deadly at high concentrations. Zn intoxication of *S. pneumoniae* results from a deficiency in Mn, which is required for key metabolic enzymes and defense against oxidative stress. Here, we report our identification and characterization of the function of the five homologous, CiaRH-regulated Ccn sRNAs in controlling *S. pneumoniae* virulence and metal homeostasis. We show that deletion of all five *ccn* genes (*ccnA*, *ccnB*, *ccnC*, *ccnD*, and *ccnE*) from *S. pneumoniae* strains D39 (serotype 2) and TIGR4 (serotype 4) causes Zn hypersensitivity and an attenuation of virulence in a murine invasive pneumonia model. We provide evidence that addition of Zn disproportionately impairs Mn uptake by the Δ*ccnABCDE* mutants. Consistent with a response to Mn starvation, expression of genes encoding the CzcD Zn exporter and the Mn-independent ribonucleotide reductase, NrdD-NrdG, were increased in the Δ*ccnABCDE* mutant relative to its isogenic *ccn*$^+$ parent strain. The growth inhibition by Zn that occurs as the result of loss of the *ccn* genes is rescued by supplementation with Mn or Oxyrase™, a reagent that removes dissolved oxygen. Lastly, we found that the Zn-dependent growth inhibition of the Δ*ccnABCDE* strain was not altered by deletion of *sodA*, whereas the *ccn*$^+$ Δ*sodA* strain phenocopied the Δ*ccnABCDE* strain. Overall, our results indicate that the Ccn sRNAs have a crucial role in preventing oxidative stress in *S. pneumoniae* during exposure to excess Zn by modulating Mn uptake.

AUTHOR SUMMARY

Zn and Mn are essential micronutrients for many bacteria, including *Streptococcus pneumoniae*. While Zn performs vital structural or catalytic roles in certain proteins, in excess, Zn can inhibit Mn uptake by *S. pneumoniae* and displace, but not functionally replace Mn from key enzymes including superoxide dismutase A (SodA). Here, we show that the Ccn small regulatory RNAs

52 promote *S. pneumoniae* Mn uptake and resistance to the oxidative stress. Furthermore, we
53 demonstrate that these small regulatory RNAs modulate the ability of *S. pneumoniae* to cause
54 invasive pneumonia. Altogether, these findings reveal a new layer of regulation of *S. pneumoniae*
55 Zn and Mn homeostasis and suggest that there are factors in addition to known transporters that
56 modulate intracellular Mn levels.
57

58 **INTRODUCTION**

59 Small regulatory RNAs have been established as fundamental regulators of gene expression in
60 bacteria and are involved in controlling nearly every aspect of bacterial physiology, metabolism,
61 and behavior (*1-3*). Two basic classes of small regulatory RNAs have been identified and
62 characterized, those that control gene expression by directly interacting with transcripts via
63 hydrogen bonding between complementary or wobble base-pairs and others that indirectly
64 effect transcript abundance by titrating an RNA or DNA-binding protein (*4, 5*). Interactions
65 between the former class of riboregulators, henceforth referred to as sRNAs, and their cognate
66 target transcripts can result in changes in their transcription, translation, and/or stability
67 depending on many factors include the sequence, accessibility, structure, and location of the
68 sRNA binding site. One of the most facile modes of regulation discovered involves the sRNA
69 binding within or adjacent to the translation initiation region blocking the 16S rRNA within the
70 30S ribosomal subunit from base-pairing with the complementary Shine-Delgarno sequence, or
71 ribosome binding site, within the mRNA. Many other elegant mechanisms of sRNA-based gene
72 regulation have been uncovered (*6-8*). While a large amount of progress has been made
73 towards understanding the contribution of sRNAs to the response of Gram-negative bacteria
74 such as *Escherichia coli* to internally and externally derived stresses, environmental cues, and
75 host interactions, much less headway has been achieved in understanding the functions of
76 sRNAs in Gram-positive bacteria, particularly, *Streptococcus pneumoniae*.

77 The Gram-positive, ovoid diplococcus *S. pneumoniae* is a leading cause of lower respiratory
78 infection morbidity and mortality worldwide resulting in nearly 2 million deaths per year (*9*). We
79 and others have discovered 100s of putative sRNAs in *S. pneumoniae* (*10-15*), but the functions
80 of almost all of them remains a mystery. Among the first sRNAs identified in *S. pneumoniae*
81 were the five homologous Ccn sRNAs (CcnA, CcnB, CcnC, CcnD, and CcnE), which were
82 shown to be transcribed in response to activation of the CiaRH two-component system (*15, 16*);
83 expression of the CiaRH two-component systems is induced by penicillin and sialic acid (*17,*
84 *18*). Shortly after the discovery of the five Ccn sRNAs, Tsui, Mukerjee (Sinha), et al
85 demonstrated that CcnA negatively regulates competence and the *comCDE* mRNA encoding
86 the precursor of the competence stimulating peptide and the two-component system that
87 responds to this signal and activates competence (*15*). Schnorpfeil et al then formally
88 demonstrated that the five Ccn sRNAs negatively regulate competence by base-pairing with the
89 *comCDE* mRNA (*19*). Other likely targets post-transcriptionally regulated by the Ccn sRNAs
90 were identified in that study including mRNAs encoding components of a galactose transporter
91 (*spd_0090*), a formate-nitrate transporter (*nirC*), branched-chain amino acid transporter (*brnQ*)
92 and a toxin *(shetA*), but direct regulation of these targets by the Ccn sRNAs has not yet been
93 shown (*19*). One of these five homologous sRNAs, CcnE, has also been implicated in *S.*
94 *pneumoniae* virulence in a murine invasive pneumonia model (*12*).
95 Here, we report our discovery of a role for the five Ccn sRNAs in controlling *S. pneumoniae*
96 virulence and Zn resistance. Specifically, we show that deletion of the genes encoding the five
97 Ccn sRNAs attenuates the virulence of *S. pneumoniae* strains D39 and TIGR4 in a murine
98 invasive pneumonia model. Additionally, we show that loss of the Ccn sRNAs leads *S.*
99 *pneumoniae* D39 and TIGR4 to become hypersensitive to Zn toxicity. Altogether, our results
100 indicate that the Ccn sRNAs promote Mn uptake leading into increased Zn resistance due to an
101 increase in the amount of active superoxide dismutase A (SodA).
102

103 **RESULTS**

104 **The Ccn sRNAs are important for *S. pneumoniae* pathogenesis.** Work from a prior study (*12*)
105 indicated that deletion of one of the five Ccn sRNA genes (*ccnE*) reduced *S. pneumoniae* serotype
106 4 strain TIGR4 virulence in a murine invasive pneumoniae model. In that study, the authors also
107 discovered by Tn-seq that transposon insertions in *ccnE* reduced *S. pneumoniae* strain TIGR4
108 fitness in murine lungs, whereas transposon insertions in *ccnA* had no significant impact on its
109 fitness in the murine lung, nasopharynx, or blood. To determine the contribution of the Ccn sRNAs
110 to the virulence of the *S. pneumoniae* serotype 2 strain D39 in a murine invasive pneumonia
111 model, we initially made single deletions of *ccnA*, *ccnB*, *ccnC, ccnD*, or *ccnE* and a quintuple
112 deletion of all five *ccn* genes in a strain background harboring the *rpsL1* allele (IU1781). Next, we
113 evaluated the growth of these strains in BHI broth at 37°C in an atmosphere of 5% CO_2. Neither
114 deletion of any single Ccn sRNA gene or all five of them had any significant effect on growth rate,
115 although the growth yield of the Δ*ccnE* strain was slightly reduced (Figs. 1A, S1A, and S1C). We
116 then determined the consequence of these deletions on *S. pneumoniae* pathogenicity in a murine
117 invasive pneumonia model (see Materials and Methods). While removal of any single *ccn* gene
118 had no significant impact on its virulence in mice (Fig. S2), deletion of all five *ccn* genes attenuated
119 *S. pneumoniae* strain D39 pathogenicity increasing median survival time from 43 h to 67 h (Fig.
120 2A).

121 To confirm that the *ccn* genes are generally important for *S. pneumoniae* virulence and is not
122 an attribute specific to strain D39, we also deleted all five *ccn* genes from a serotype 4 TIGR4
123 strain harboring the *rpsL1* allele (NRD10220) and measured the impact of these deletions on its
124 growth and virulence using the same murine invasive pneumonia model. As shown in Fig. 1D,
125 deletion of all five *ccn* genes did have an effect on growth rate of *S. pneumoniae* TIGR4 in BHI
126 broth incubated at 37°C with an atmosphere of 5% CO_2. To validate the effect of the *ccnABCDE*
127 deletion on *S. pneumoniae* TIGR4 growth, we reconstructed the quintuplet deletion strain from
128 scratch, but this time we subsequently replaced the mutant *rpsL* allele conferring streptomycin

129 resistance that aided in construction of the unmarked deletions of the *ccn* genes back to the wild
130 type *rpsL* allele. Next, we tested the growth of that strain and its parental *ccn*$^+$ TIGR4 strain in BHI
131 broth at 37°C under an atmosphere of 5% CO_2. Again, we saw a substantial reduction in growth
132 rate when all five *ccn* genes were deleted (Fig. S3A). The *ccnABCDE* deletion also resulted in a
133 marked attenuation of *S. pneumoniae* TIGR4 virulence increasing the survival rate of ICR outbred
134 mice from 0% to 50% (Fig. 2B). Two of the mice that survived infection with the TIGR4
135 Δ*ccnABCDE* strain had no detectable bacteria in the blood and the other two mice had 1000 and
136 2750 CFUs per mL of blood, respectively, which was far below 10^7 bacteria found in moribund
137 mice that were infected with the *ccn*$^+$ parent strain. Our results show that the *ccn* genes are
138 important for *S. pneumoniae* pathogenesis.
139
140 **The Ccn sRNAs impact expression of Zn and Mn-related genes.** To discover a basis for the
141 defect in *S. pneumoniae* virulence caused by the deletion of the five *ccn* genes, we compared
142 global gene expression by high throughput RNA-sequencing (RNA-seq) between *S. pneumoniae*
143 strain D39 or TIGR4 and the derived Δ*ccnABCDE* mutant strains grown to exponential phase
144 (OD_{620} between 0.15 and 0.2) in BHI broth at 37°C in an atmosphere of 5% CO_2. In the *S.*
145 *pneumoniae* D39 strain background, the *ccnABCDE* deletion resulted in down-regulation of 3
146 genes and up-regulation of 113 genes by 2-fold or more ($P_{adj} < 0.05$) (Table S3). In contrast,
147 deletion of the *ccn* genes from the TIGR4 strain resulted in down-regulation of 25 genes and up-
148 regulation of 97 genes by 2-fold or greater ($P_{adj} < 0.05$) (Table S4). 37 genes were up-regulated
149 by 2-fold ($P_{adj}<0.05$) in the *ccnABCDE* deletion strain in both the D39 and TIGR4 backgrounds
150 (Table 1); among these differentially expressed genes were iron uptake system genes (*piuB*,
151 *piuC*, *piuD*, and *piuA*), a Zn-responsive ECF (energy-coupling factor) transport gene
152 SPD_1267/SP_1438, and *czcD* encoding a Zn/Cd exporter that provides Zn and Cd resistance.
153 To validate our RNA-seq data, we first measured abundance of *piuB*, *spd_1267*, and *czcD*

154 transcripts in RNA samples isolated for the RNA-seq experiment from *S. pneumoniae* strain D39
155 and derived Δ*ccnABCDE* strain by reverse transcriptase droplet digital PCR (RT-ddPCR).
156 Consistent with our RNA-seq data the *piuB, spd_1267,* and *czcD* transcripts were up-regulated
157 by 3.47, 10.5, and 1.93-fold respectively in the Δ*ccnABCDE* strain compared to its parental D39
158 strain grown in BHI broth (Fig. 3A, B, and C). Using RT-ddPCR analysis of the RNA samples
159 isolated from exponential cultures of *S. pneumoniae* TIGR4 and derived Δ*ccnABCDE* mutant
160 strain grown in BHI broth at 37°C under an atmosphere of 5% CO_2, we also observed a 2.45
161 increase in the abundance of the *czcD* mRNA in the *ccn* mutant as compared to its parental strain
162 (Fig. 3E). Altogether, these data suggested to us that removal of the *ccn* genes from *S.*
163 *pneumoniae* was leading to an increase in the intracellular abundance of Zn relative to Mn, and
164 to cope with this stress, the *ccn* mutant strain was increasing expression of the CzcD Zn exporter.
165

166 **Table 1: Genes significantly, differentially expressed between a Δ*ccnABCDE* and *ccn*⁺**
167 **strain in both the *S. pneumoniae* D39 and TIGR4 background during exponential growth**
168 **in BHI broth[a]**

D39 locus tag	Gene	Known or predicted function	D39 fold change	TIGR4 fold change
SPD_0025		tRNA-specific adenosine-34 deaminase	84.3	144
SPD_0027	*dut*	deoxyuridine 5'-triphosphate nucleotidohydrolase	3.52	4.39
SPD_0028		hypothetical protein	3.80	3.40
SPD_0029	*radA*	DNA repair protein	3.55	2.80
SPD_0090		galactose ABC transport protein	2.09	2.00
SPD_0104		aggregation-promoting factor	2.69	2.27
SPD_0222	*gpmB1*	phosphoglycerate mutase family protein	25.0	22.9
SPD_0243	*uppS*	undecaprenyl diphosphate synthase	5.97	4.42
SPD_0244	*cdsA*	phosphatidate cytidylyltransferase	5.50	4.49
SPD_0245	*eep*	intramembrane protease	5.57	4.19
SPD_0246	*proS*	prolyl-tRNA synthetase	5.91	4.68
SPD_0247	*bglA*	6-phospho-β-glucosidase	3.57	3.35
SPD_0308	*clpL*	ATP-dependent protease subunit	13.7	2.71
SPD_0460	*dnaK*	protein chaperone	3.97	2.01
SPD_0501	*licT*	β-glucoside operon antiterminator	2.91	4.77
SPD_0502	*bglF*	β-glucoside PTS transporter subunit	3.07	5.65

SPD_0503	*bglA-2*	6-phospho- β-glucosidase	2.57	4.79
SPD_0615	*glnH3*	degenerate glutamine ABC transporter subunit	11.6	4.05
SPD_0616	*glnQ3*	glutamine ABC transporter subunit	8.90	3.07
SPD_0617	*glnP3b*	glutamine ABC transporter subunit	11.1	3.63
SPD_0618	*glnP3a*	glutamine ABC transporter subunit	11.8	2.98
SPD_0775		acetyltransferase	3.29	2.71
SPD_1045		degenerate DUF3884 domain protein	4.73	3.16
SPD_1046	*lacG-2*	6-phospho-β-galactosidase	3.56	2.92
SPD_1267		ECF transporter subunit	11.1	2.14
SPD_1638	*czcD*	Cd/Zn exporter	2.69	2.66
SPD_1649	*piuB*	Fe uptake transporter subunit	5.13	2.43
SPD_1650	*piuC*	Fe uptake transporter subunit	4.45	2.01
SPD_1651	*piuD*	Fe uptake transporter subunit	4.22	2.15
SPD_1652	*piuA*	Fe uptake transporter subunit	4.38	2.25
SPD_1748	*pneA2*	lantibiotic peptide	2.19	2.16
SPD_1749	*lanM*	lanthionine biosynthesis protein	2.49	2.29
SPD_1750	*wrbA*	FAD-dependent flavoprotein	3.00	2.69
SPD_1751		hypothetical protein	2.56	3.16
SPD_1752	*clyB*	toxin secretion ABC transporter	3.58	3.22
SPD_1753		epidermin leader peptide processing serine protease	2.44	2.87
SPD_1932	*malP*	malodextrin phosphorylase	2.58	2.58

[a]RNA extraction and mRNA-seq analyses were performed as described in *Materials and Methods*. RNA was prepared from cultures of strains IU1781 (D39 *rpsL1*), NRD10176 (D39 *rpsL1* Δ*ccnABCDE*), NRD10220 (TIGR4 *rpsL1*), and NRD10266 (TIGR4 *rpsL1* Δ*ccnABCDE*) (Table S1 and S2). Fold changes (2.0-fold cut-off) and adjusted P-values (Pval <0.05) are based on three independent biological replicates.

Absence of the *ccn* genes causes S*. pneumoniae* to become hypersensitive to Zn. If the absence of the *ccn* genes from *S. pneumoniae* leads to an imbalance of transition metals with higher levels of Zn relative to Mn, then we would expect that increasing the concentration of Zn present in the medium would disproportionately impair the growth of the Δ*ccnABCDE* mutant relative to the isogenic *ccn*$^+$ strain. Previous studies have indicated that Becton-Dickinson (BD) BHI broth typically contains ~20 μM Zn and 200 nM Mn (*20, 21*). We first compared growth of

182 strain D39 and derived Δ*ccnA*, Δ*ccnB*, Δ*ccnC*, Δ*ccnD*, Δ*ccnE*, and Δ*ccnABCDE* strains in BHI
183 broth alone or supplemented with 0.2 mM Zn at 37°C under an atmosphere of 5% CO_2. No
184 significant difference was observed in growth rate between strain D39 and derived Δ*ccnA*, Δ*ccnB*,
185 Δ*ccnC*, and Δ*ccnD* mutant strains in BHI in the presence or absence of 0.2 mM added Zn (Fig.
186 S1), although the growth yield for the *ccnE* mutant was lower in BHI in the presence and absence
187 of Zn. As noted above, growth the strain D39 and derived Δ*ccnABCDE* mutant strain was similar
188 in BHI broth alone (Fig. 1A.) In contrast, the absence of all five *ccn* genes led to an obvious
189 impairment in growth rate in BHI supplemented with 0.2 mM Zn (Fig. 1B) This growth deficiency
190 relative to the *ccn*$^+$ parental strain was also observed for the Δ*ccnABCDE* strain when Zn was
191 increased in BHI broth to 0.4 mM (Fig. 1C). Consistently, addition of Zn at 0.4 mM severely
192 reduced the growth rate of the *ccn*$^+$ D39 strain. Reintroduction of *ccnC* and *ccnD* expressed from
193 their native promoters at ectopic loci partially ameliorated the growth defect of the Δ*ccnABCDE*
194 mutant strain in BHI supplemented with 0.2 mM or 0.4 mM Zn, whereas insertion of copies of
195 *ccnA, ccnB*, and *ccnD* with their native promoter at the *bgaA* and CEP loci completely corrected
196 the growth deficiency of this quintuple *ccn* mutant (Figs. 1B and 1C) under these growth
197 conditions. To verify that the Zn hypersensitivity caused by the deletion of all five *ccn* genes was
198 not specific to the serotype 2 strain D39, we also tested the effect of the quintuple *ccn* deletion on
199 the growth of the serotype 4 TIGR4 strain in BHI broth supplemented with Zn. Consistent with our
200 results observed for strain D39, deletion of the Ccn sRNA genes from TIGR4 led to a growth
201 impairment in BHI when Zn was added at a final concentration of 0.2 or 0.4 mM (Figs. 1D-F and
202 S3). Curiously, Zn at the highest concentration used had less of an effect on TIGR4 growth than
203 it did on the D39 strain. Overall, these results indicate that Ccn sRNAs promote *S. pneumoniae*
204 Zn tolerance.
205

206 **The Zn-hypersensitivity that occurs in the absence of the Ccn sRNA genes is due to a**
207 **reduction in cellular Mn levels.** *S. pneumoniae* is a Mn-centric bacteria encoding several Mn-
208 requiring enzymes including superoxide dismutase (SodA), a capsule regulatory kinase (CpsB),
209 phosphoglucomutase (Pgm), phosphopentomutase (DeoB), a cell division regulating
210 phosphatase (PhpP), an aerobic ribonucleotide reductase (NrdEF), pyruvate kinase (PyK), and
211 lactate dehydrogenase (Ldh). Mis-metalation of these Mn-dependent enzymes by Zn, which
212 inhibits their enzymatic activity (*22, 23*), can occur when the internal ratio of Zn-to-Mn is high.
213 Additionally, the substrate binding component of the PsaBCA Mn ATP binding cassette (ABC)
214 type transporter, the only known Mn importer in *S. pneumoniae*, has been shown to bind Zn tightly,
215 blocking Mn uptake (*20, 24*). Our RNA-seq and RT-ddPCR data above indicated that expression
216 of the CzcD Zinc exporter, which is expressed in response to high levels of Zn relative to Mn (*25,*
217 *26*), is up-regulated in *S. pneumoniae* strains lacking the *ccn* genes (Fig. 3C and E). Based on
218 these results and the published data mentioned above, we hypothesized that Zn-hypersensitivity
219 caused by the removal of all five *ccn* genes from the *S. pneumoniae* genome is due to reduced
220 Mn uptake. If this postulate is correct, then the Zn-dependent growth inhibition that occurs when
221 the *S. pneumoniae* Δ*ccnABCDE* mutant strain is grown in BHI broth supplemented with 0.2 mM
222 Zn should be rescued by inclusion of an equimolar amount of Mn into the medium. As shown in
223 Fig. 4, the growth impairment of the Δ*ccnABCDE* mutant of *S. pneumoniae* D39 or TIGR4 strain
224 in BHI broth with 0.2 mM Zn is cured by addition of 0.2 mM Mn consistent with our model.
225 To directly test whether or not the levels of transition metals are perturbed in strains lacking
226 the *ccn* genes, we measured total cell associated transition metals in *S. pneumoniae* strain D39,
227 derived Δ*ccnABCDE* mutant, and the Δ*ccnABCDE* strain complemented with *ccnA*, *ccnB*, and
228 *ccnD* by inductively coupled plasma-mass spectrometry (ICP-MS). During exponential growth
229 (OD_{620} of ~0.2) in BHI broth alone or supplemented with 0.2 mM Zn, there was no significant
230 difference in Zn abundance among these strains (Fig 5A). Similarly, Mn levels were comparable

231 among all tested strains when grown to exponential phase in BHI broth alone (Fig. 5B). However,
232 there was a modest, but statistically significant (P = 0.039), 22% reduction in total cell associated
233 Mn in the Δ*ccnABCDE* mutant compared to its parental *ccn*$^+$ strain, which was partially
234 complemented by *ccnA*, *ccnB*, and *ccnD*. Thus, our evidence that Mn supplementation eliminated
235 the growth deficiency of the *ccn*$^-$ strain caused by excess Zn and that the amount of Mn associated
236 with this mutant strain was reduced compared to the *ccn*$^+$ strain when exposed to a high Zn
237 concentration suggest that the Ccn sRNAs are important for preserving Mn homeostasis, when
238 *S. pneumoniae* encounters a Zn-rich environment.
239
240 **Oxidative stress due to reduced levels of active superoxide dismutase A contributes to the**
241 **Zn hypersensitivity of the *S. pneumoniae* strain lacking the Ccn sRNAs.** To discover the
242 molecular basis for the Zn hypersensitivity caused by loss of the *ccn* genes, we turned to an RNA-
243 seq based approach. Briefly, we compared transcript abundance in RNA isolated from *S.*
244 *pneumoniae* strain D39 and derived Δ*ccnABCDE* strain grown to exponential phase (OD_{620} of
245 ~0.2) at 37°C under an atmosphere of 5% CO_2 in BHI broth supplemented with 0.2 mM Zn. Similar
246 to our RNA-seq performed with these strains in the absence of Zn supplementation, we observed
247 a 2.33-fold increase in expression of the CzcD Zn exporter specifying mRNA and a 9.5-fold
248 increase in the Spd_1267 Zn-responsive ECF-type transporter producing mRNA in the
249 Δ*ccnABCDE* mutant compared to its *ccn*$^+$ parent strain (Tables 2 and S5). Interestingly, we also
250 saw a 1.90-fold decrease (P_{adj} = 1.81x10^{-43}) in expression of the *sodA* mRNA, encoding
251 superoxide dismutase A, in the Δ*ccnABCDE* mutant strain, which was just below our arbitrary
252 two-fold cutoff (Table S5). We subsequently measured the relative abundance of these transcripts
253 by RT-ddPCR and northern blot analysis (Figs. 3B, C, and D) and were able to confirm our RNA-
254 seq results indicating up-regulation of *spd_1267* and *czcD* mRNAs and down-regulation of the
255 *sodA* mRNA abundance when the *ccn* genes were deleted from *S. pneumoniae*. This result was

256 intriguing to us since a prior study found that Mn starvation of *S. pneumoniae* cells due to
257 exposure to high concentrations of Zn relative to Mn led to a reduction in the transcription of *sodA*
258 and a reduction in superoxide dismutase activity (*22*). Furthermore, Eijkelkamp *et* al discovered
259 that deletion of *sodA* had no significant impact on *S. pneumoniae* growth under Mn replete
260 conditions, but was vital for growth in media containing a high Zn-to-Mn ratio (*22*).
261
262 **Table 2: Genes significantly, differentially expressed between a *S. pneumoniae* D39 and**
263 **derived Δ*ccnABCDE* strain in both BHI alone or supplemented with Zn[a]**

D39 locus tag	Gene	Known or predicted function	Fold change (BHI)	Fold change (BHI+Zn)
SPD_0025		tRNA-specific adenosine-34 deaminase	84.3	49.0
SPD_0027	*dut*	deoxyuridine 5'-triphosphate nucleotidohydrolase	3.52	3.76
SPD_0028		hypothetical protein	3.80	3.02
SPD_0029	*radA*	DNA repair protein	3.55	2.95
SPD_0080	*pavB*	cell wall surface anchor family protein	6.69	6.32
SPD_0163		DNA binding protein	2.00	2.07
SPD_0222	*gpmB1*	phosphoglycerate mutase family protein	25.0	21.7
SPD_0243	*uppS*	undecaprenyl diphosphate synthase	5.97	7.61
SPD_0244	*cdsA*	phosphatidate cytidylyltransferase	5.50	7.77
SPD_0245	*eep*	intramembrane protease	5.57	8.59
SPD_0246	*proS*	prolyl-tRNA synthetase	5.91	9.65
SPD_0247	*bglA*	6-phospho-β-glucosidase	3.57	4.73
SPD_0277	*bglA-1*	6-phospho-β-glucosidase	3.53	2.73
SPD_0279	*celB*	cellobiose PTS transporter subunit	5.05	2.97
SPD_0308	*clpL*	ATP-dependent protease subunit	13.7	9.55
SPD_0350	*vraT*	cell wall-active antibiotic response protein	2.19	2.62
SPD_0351	*vraS*	two-component system histidine kinase	2.29	2.74
SPD_0352	*vraR*	two-component system response regulator	2.31	2.70
SPD_0353	*alkD*	degenerate DNA alkylation repair enzyme	2.11	2.67
SPD_0354	*alkD*	degenerate DNA alkylation repair enzyme	2.37	2.69
SPD_0458	*hrcA*	heat inducible transcription repressor	3.62	3.69
SPD_0459	*grpE*	heat shock protein	3.77	3.87
SPD_0460	*dnaK*	protein chaperone	3.97	3.82
SPD_0461	*dnaJ*	protein chaperone	3.50	3.52
SPD_0474	*blpZ*	immunity protein	2.40	2.05
SPD_0501	*licT*	β-glucoside operon antiterminator	2.91	5.26
SPD_0502	*bglF*	β-glucoside PTS transporter subunit	3.07	4.65
SPD_0503	*bglA-2*	6-phospho- β-glucosidase	2.57	3.75
SPD_0537		putative Zn-dependent protease	2.07	2.21

SPD_0615	*glnH3*	degenerate glutamine ABC transporter subunit	11.6	18.0
SPD_0616	*glnQ3*	glutamine ABC transporter subunit	8.90	16.8
SPD_0617	*glnP3b*	glutamine ABC transporter subunit	11.1	15.8
SPD_0618	*glnP3a*	glutamine ABC transporter subunit	11.8	15.1
SPD_0681		hypothetical protein	2.82	5.45
SPD_0701	*ciaR*	two-component response regulator	2.72	2.56
SPD_0702	*ciaH*	two-component histidine kinase	2.80	3.01
SPD_0775		acetyltransferase	3.29	3.61
SPD_0803		putative phage shock protein C		
SPD_0804		ABC transporter ATP-binding protein	2.28	3.01
SPD_0805		ABC transporter permease protein	2.43	3.15
SPD_0913		extracellular protein	3.39	3.31
SPD_0938		degenerate TN5252 relaxase	9.35	5.06
SPD_0940	*rrfD*	UDP-N-acetyl-D-mannosaminouronic acid dehydrogenase.	3.95	5.31
SPD_0942		hypothetical protein	2.25	2.41
SPD_0943		hypothetical proein	2.41	2.43
SPD_0944		nodulation protein L	2.24	2.38
SPD_0946		hypothetical protein	2.16	3.27
SPD_0947		hypothetical protein	2.69	3.97
SPD_0948	*nikS*	nikkomycin biosynthesis protein	3.73	4.29
SPD_0949		N-acetylneuraminate synthase	2.38	4.85
SPD_0950	*mefE*	macrolide ABCE transporter subunit	2.44	3.99
SPD_1045		degenerate DUF3884 domain protein	4.73	6.81
SPD_1046	*lacG-2*	6-phospho-b-galactosidase	3.56	7.28
SPD_1047	*lacE-2*	lactose PTS transporter subunit	4.21	6.33
SPD_1049	*lacT*	β-glucoside *bgl* operon antiterminator	3.23	3.48
SPD_1114		hypothetical protein	13.5	5.37
SPD_1267		ECF transporter subunit	11.1	9.53
SPD_1297	*pdxS*	pyridoxal 5'-phosphate synthase	2.02	2.04
SPD_1506	*axe1*	acetyl xylan esterase 1	3.62	2.68
SPD_1615		degenerate hypothetical protein	4.02	2.09
SPD_1638	*czcD*	Cd/Zn exporter	2.69	2.33
SPD_1709	*groL*	HSP60 family chaperone	2.58	2.38
SPD_1710	*groES*	HSP60 family chaperone	2.25	2.31
SPD_1716		hypothetical protein	2.56	5.62
SPD_1717		membrane protein	2.40	5.22
SPD_1718		LytR/AlgR family response regulator	2.44	4.58
SPD_1746		hypothetical protein	2.96	4.25
SPD_1747	*pneA1*	lantibiotic peptide	2.02	4.29
SPD_1748	*pneA2*	lantibiotic peptide	2.19	4.60
SPD_1749	*lanM*	lanthionine biosynthesis protein	2.49	2.37
SPD_1750	*wrbA*	FAD-dependent flavoprotein	3.00	2.85
SPD_1751		hypothetical protein	2.56	4.07
SPD_1752	*clyB*	toxin secretion ABC transporter	3.58	4.02
SPD_1753		epidermin leader peptide processing serine protease	2.44	3.00
SPD_1769		membrane protein	2.29	3.42

SPD_1932	*malP*	malodextrin phosphorylase	2.58	2.95
SPD_1933	*malQ*	4-α-glucanotransferase	2.76	2.77
SPD_1990		mannose PTS transporter subunit	2.01	13.8
SPD_1994	*fucA*	L-fuculose phosphate aldolase	2.35	8.69
SPD_2034	*comFC*	phosphororibosyltransferase domain protein	32.7	14.1
SPD_2035	*comFA*	DNA transporter ATPase	8.88	10.2
SPD_2068	*htrA*	serine protease	2.79	2.13
SPD_2069	*parB*	chromosome partitioning protein	3.04	2.88

264

265 [a]RNA extraction and mRNA-seq analyses were performed as described in *Materials and Methods*.
266 RNA was prepared from cultures of strains IU1781 (D39 *rpsL1*) and NRD10176 (D39 *rpsL1*
267 Δ*ccnABCDE*) grown to exponential phase in BHI alone or supplemented with 0.2 mM $ZnSO_4$
268 (Table S1 and S2). Fold changes (2.0-fold cut-off) and adjusted P-values (Pval <0.05) are based
269 on three independent biological replicates.

270

271 To initially examine whether the growth deficiency of the Δ*ccnABCDE* mutant relative to the
272 *ccn*$^+$ D39 strain was due in part to oxidative stress, we evaluated the impact of addition of
273 Oxyrase™, an enzyme mixture that removes molecular oxygen by reducing it to water, on the
274 growth of these strains in BHI broth alone or supplemented with 0.2 mM or 0.4 mM Zn (Fig 6A, B,
275 and C) under an atmosphere of 5% CO_2. Once again, we observed that deletion of *ccnA*, *ccnB*,
276 *ccnC*, *ccnD*, and *ccnE* from *S. pneumoniae* strain D39 had no significant impact on growth in BHI
277 alone. However, under these growth conditions, the addition of Oxyrase™ reduced the growth
278 rate of both the *ccn*$^+$ and ccn$^-$ strains to a similar extent (Fig. 6A). As we anticipated, addition of
279 Oxyrase™ to BHI supplemented with Zn (0.2 mM) improved the growth rate of the Δ*ccnABCDE*
280 strain to that observed for the *ccn*$^+$ D39 parent strain (Fig. 6B). Interestingly, addition of Oxyrase™
281 improved the growth rate of both strains in BHI with 0.4 mM Zn and eliminated any growth
282 differences between them (Fig. 6C). Finally, we examined the contribution of *sodA* to the growth
283 of *S. pneumoniae* D39 and derived Δ*ccnABCDE* mutant strain. In BHI broth alone or
284 supplemented with 0.2 mM Zn, deletion of *sodA* reduced the growth rate of the *ccn*$^+$ strain, but

285 had no significant reduction in growth rate of the Δ*ccnABCDE* mutant strain (Fig. 7). Based on
286 these results, we concluded that the amount of functional SodA was negligible in the *S.*
287 *pneumoniae* strain lacking the Ccn sRNAs and thus, deleting *sodA* did not significantly impact its
288 growth, whereas this deletion does substantially impair growth of the isogenic *ccn*$^{+}$ strain.
289

290 **DISCUSSION**

291 High density Tn-seq experiments performed more than a decade ago revealed that sRNAs
292 play a crucial role in regulating *S. pneumoniae* virulence including its ability to colonize the blood,
293 nasopharynx, and lungs of its host (*12*). While this discovery in itself may not be surprising, it is
294 astonishing that very little progress has been made towards understanding the functions of these
295 sRNAs given their importance in governing *S. pneumoniae* pathogenesis. Here, we investigated
296 the contribution of the five homologous Ccn sRNAs to *S. pneumoniae* pathogenesis and gene
297 regulation. Not only have we confirmed their crucial role in pneumococcal disease progression
298 (Fig. 2), but also discovered their extensive functions in regulating gene expression and Zn
299 resistance. Specifically, we found that exposure to relatively high, yet host-relevant, Zn
300 concentrations (0.2 mM) disproportionally inhibited growth (Fig 1, 4, 6, and 7) and modestly
301 reduced total cell associated Mn levels (Fig. 5) of *S. pneumoniae* strains lacking genes for the
302 five Ccn sRNAs. This Zn-dependent growth inhibition caused the *ccnABCDE* deletion was
303 completely alleviated by addition of Mn (Fig. 4) or Oxyrase™ (Fig. 6), which removes molecular
304 oxygen by reducing it to water. Furthermore, deletion of *sodA*, encoding the Mn-dependent
305 superoxide dismutase A, from *S. pneumoniae* resulted in a Zn-dependent growth inhibition
306 indistinguishable from that observed for the Δ*ccnABCDE* strain; however, the same deletion had
307 no impact on the growth of the Δ*ccnABCDE* strain (Fig. 7). Altogether, these results indicate that
308 the Ccn sRNAs promote Mn uptake and availability resulting in an increased abundance of active

309 SodA, which improves the growth of *S. pneumoniae* in a Zn-rich environment due to greater
310 protection from damaging reactive oxygen species.

311 How do the Ccn sRNAs promote an increased concentration of free intracellular Mn^{2+} cations?
312 Potential mechanisms through which the Ccn sRNAs could increase the concentration of
313 available Mn inside *S. pneumoniae* cells include that the Ccn sRNAs (1) negatively regulate
314 expression of a Mn exporter, (2) positively regulate expression of a Mn importer, (3) reduce
315 production of an intracellular protein or other factor that effectively chelates Mn, or (4) decrease
316 synthesis of a cellular component that would otherwise restrict access of Mn to the periplasmic
317 Mn binding component of the Mn importer. The main Mn exporter of *S. pneumoniae* is MntE (Fig.
318 8), as deletion of the encoding gene leads to accumulation of total cell associated Mn (*21, 27*).
319 MgtA, designated as a Ca efflux protein, appears to also export Mn, but has a very limited role in
320 this process (Fig. 8) (*28*). Neither MntE or MgtA were up-regulated in either *S. pneumoniae* strain
321 D39 or TIGR4 when the *ccn* genes were deleted (Tables S3 S4, and S5) making it unlikely that
322 the Ccn sRNAs increase intracellular Mn levels by down-regulating expression of these Mn
323 exporter genes. Additionally, we were unable to identify strong Ccn sRNA binding sites in the
324 translation initiation region of *mntE* or *mgtA*, which suggests that these sRNAs do not regulate
325 translation of these transcripts. Finally, if the Ccn sRNAs increase total cell-associated Mn levels
326 by down-regulating MntE expression, then we would expect that deletion of *mntE* would suppress
327 the Zn hypersensitivity of the *S. pneumoniae* Δ*ccnABCDE* mutant; however, this did not occur
328 (Fig S4A and C).

329 An alternative possibility is that the Ccn sRNAs promote Mn uptake by positively regulating
330 expression of the *psaBCA* operon encoding the only known Mn importer in *S. pneumoniae* (Fig.
331 8)(*29, 30*). Localized to the inner membrane, PsaB is the ATP binding component whereas PsaC
332 is the permease of this ABC-type transporter. PsaA, the substrate binding component, is located
333 in the periplasm, where it binds Mn. Once again, in our RNA-seq experiments, we did not observe
334 a decrease in expression of the *psaBCA* operon when the *ccn* genes were deleted from *S.*

335 *pneumoniae* strain D39 or TIGR4 (Tables S3, S4, and S5) indicating that the Ccn sRNAs do not
336 positively regulate expression of this Mn importer. Furthermore, if this was the case, then we
337 would expect that deletion of *psaR* encoding the repressor of the *psaBCA* operon (*31, 32*) might
338 suppress the Zn-dependent growth inhibition of the *S. pneumoniae* Δ*ccnABCDE* mutant;
339 however, we did not observe this (Fig. S4B and D).

340 While it remains possible that the Ccn sRNAs regulate production of a factor that chelates
341 intracellular Mn, we did not observe the up-regulation of any *known* Mn-binding proteins via RNA-
342 seq. A final possibility that we surmised could be occurring is that the Ccn sRNAs negatively
343 impact the production or architecture of a structure that could restrict Mn uptake by limiting the
344 diffusion of Mn into the periplasm, where it could be transported by the PsaBCA Mn importer into
345 the cytoplasm. For example, a physical structure that might serve as a permeability barrier to Mn
346 is the polysaccharide capsule that surrounds *S. pneumoniae* diplococci. To test this possibility,
347 we evaluated the impact of deleting the capsule biosynthetic genes on the Zn hypersensitivity of
348 the *S. pneumoniae* Δ*ccnABCDE* mutant. Interestingly, we observed that the *cps2ABCDETFGH*
349 deletion completely suppressed the Zn hypersensitivity of an *S. pneumoniae* strain lacking the
350 *ccn* genes (Fig. S4C and F). While the *ccnABCDE* deletion did not cause *S. pneumoniae* to
351 express the capsule biosynthetic genes at a higher level (Tables S3 S4, and S5), we did observe
352 increased expression of genes in the Leloir pathway (*galK* and *galT2*), which is involved in the
353 synthesis of a precursor for capsular polysaccharide synthesis (UDP-glucose), in the Δ*ccnABCDE*
354 mutant as compare to its isogenic *ccn*$^+$ parental D39 strain when grown in BHI broth
355 supplemented with 0.2 mM $ZnSO_4$ (Table S5 and Fig. 8). Notably, increased production of
356 capsular polysaccharide precursors has been shown to increase capsule production (*33, 34*). In
357 future studies, we plan on rigorously testing this model that the Ccn sRNAs decrease capsule
358 synthesis by reducing expression of genes involved in synthesizing capsular polysaccharide

359 precursors leading to an increase in Mn uptake (Fig. 8). Moreover, we intend to evaluate the
360 molecular mechanism by which the Ccn sRNAs regulate expression of these genes.
361
362 **MATERIALS AND METHODS**
363 **Bacterial strains and growth conditions.** Bacterial strains used in this study were derived
364 from encapsulated *S. pneumoniae* serotype 2 strain D39W (*14*) and TIGR4 and are listed in Table
365 S1. Strains were grown on plates containing trypticase soy agar II (modified; Becton-Dickinson
366 [BD]) and 5% (vol/vol) defribrinated sheep blood (TSAII BA) at 37°C in an atmosphere of 5% CO_2,
367 and liquid cultures were statically grown in BD brain heart infusion (BHI) broth at 37°C in an
368 atmosphere of 5% CO_2. Bacteria were inoculated into BHI broth from frozen cultures or single,
369 isolated colonies. For overnight cultures, strains were first inoculated into a 17-mm-diameter
370 polystyrene plastic tube containing 5 mL of BHI broth and then serially diluted by 100-fold into
371 four tubes; these cultures were then grown for 10 to 16 h. Cultures with an optical density at 620
372 nm (OD_{620}) of 0.1 to 0.4 were diluted to a starting OD_{620} between 0.002 and 0.005 in 5 mL of BHI
373 broth in 16-mm glass tubes. Growth was monitored by measuring OD_{620} using a Genesys 30
374 visible spectrophotometer (ThermoFisher Scientific). For antibiotic selections, TSAII BA plates
375 and BHI cultures were supplemented with 250 µg kanamycin per mL, 150 µg streptomycin per
376 mL, or 0.3 µg erythromycin per mL.
377
378 **Construction and confirmation of mutants.** Mutant strains were constructed by
379 transformation of competent *S. pneumoniae* D39 and TIGR4 derived strains with linear PCR
380 amplicons as described previously (*35, 36*). DNA amplicons containing antibiotic resistance
381 markers were synthesized by overlapping fusion PCR using the primers listed in Table S2.
382 Competence was induced in *S. pneumoniae* D39 or TIGR4 derived cells with CSP-1 or CSP-2,
383 respectively, synthetic competence stimulatory peptide. Unmarked deletions of the target genes
384 were constructed using the *kan*^{R}-*rpsL*$^{+}$ (Janus cassette) allele replacement method as described

385 previously (*37*). In the first step, the Janus cassette containing *rpsL*$^+$ allele and a kanamycin
386 resistance gene was used to disrupt target genes in an *rpsL1* or *rpsLK56T* (Str^R) strain
387 background, and transformants were selected for kanamycin resistance and screened for
388 streptomycin sensitivity. In the second step, the Janus cassette was eliminated by replacement
389 with a PCR amplicon lacking antibiotic markers and the resulting transformants were selected for
390 streptomycin resistance and screened for kanamycin sensitivity. Freezer stocks were made of
391 each strain from single colonies isolated twice on TSAII BA plates containing antibiotics listed in
392 Table S1. All strains were validated by PCR amplification and sequencing.
393
394 **RNA extraction.** To isolate RNA, strains were grown in 30 mL of BHI starting at an OD_{620} =
395 0.002 in 50 mL conical tubes. RNA was extracted from exponentially growing cultures of IU1781
396 (D39), NRD10220 (TIGR4), and their derived isogenic mutants lacking all five *ccn* genes,
397 NRD10176 (D39 Δccn) and NRD10266 (TIGR4 Δccn), at OD_{620} ≈ 0.2 using the FastRNA Pro Blue
398 Kit (MP Bio) according to the manufacturer's guidelines. Briefly, cells were collected by
399 centrifugation at 16,000 x g for 8 min at 4°C. Cell pellets were resuspended in 1 mL of RNApro™
400 solution (MP Bio) and processed five-times for 40 sec at 400 rpm in a BeadBug™ homogenizer
401 (Benchmark Scientific). Cell debris was removed by centrifugation at 16,000 x g for 5 min at 4°C.
402 After mixing 300 μL of chloroform with the supernatant, the aqueous and organic layers were
403 separated by centrifugation at 16,000 x g for 5 min at 4°C. RNA was precipitated with 500 μL of
404 ethanol at -80°C overnight. After collecting the precipitated RNA by centrifugation at 16,000 x g
405 for 15 min at 4°C, the pellet was washed once with 75% ethanol and suspend in DEPC-treated
406 water. The amount and purity of all RNA samples isolated were assessed by NanoDrop
407 spectroscopy (Thermo Fisher).
408

409 **Library preparation and mRNA-seq.** cDNA libraries were prepared from total RNA Azenta Life
410 Sciences. Briefly, total RNA was subjected to rRNA-depletion using the FastSelect 5S/16S/23S
411 rRNA depletion kit for bacteria. Libraries were the generated with NEBNext Ultra™ II Directional
412 RNA Library Prep Kit. 150 bp paired-end read sequencing was performed using an Illumina
413 HiSeq4000 sequencer.
414
415 **RNA-seq analysis.** The raw sequencing reads were quality and adapter trimmed using Cutadapt
416 version 4.1 with a minimum length of 18 nucleotides. The trimmed reads were then mapped on
417 the *Streptococcus pneumoniae* D39 (Genbank CP000410) genome using Bowtie2 (*38*). HTseq
418 version 2.0.2 was used to generate read counts for the genes (*39*). Differential gene expression
419 was identified using the program DESeq2 with default parameters (*40*). Primary data from the
420 mRNA-seq analyses were submitted to the NCBI Gene Expression Omnibus (GEO) and have
421 the accession number GSE246655.
422
423 **Reverse transcriptase-droplet digital PCR (RT-ddPCR) analysis.** RT-ddPCR was performed
424 as described previously (*41*). Isolated RNA was treated with DNase (TurboDNase, Ambion) as
425 per manufacturer's instructions. Next, RNA (1 μg) was reverse transcribed using Superscript III
426 reverse transcriptase (Invitrogen) with random hexamers. RT and No RT control (NRT) sample
427 were utilized. These samples were diluted $1:10^1$, $1:10^2$, $1:10^3$, or $1:10^6$. Then, 2 µL of each diluted
428 RT and NRT sample was added to a 22 µL reaction mixture containing 11 µL of QX200™ ddPCR
429 ™ Evagreen Supermix (Bio-Rad) and 1.1 µL of each 2 µM ddPCR primers (Table S6). A single
430 no template control (NTC) was included for each ddPCR primer pair used. Reactions were
431 performed using at least three independent biological replicates. Droplets were generated using
432 the QX200 Automated Droplet Generator (Bio-Rad), and end-point PCR was carried out using a
433 C1000 Touch™ thermal cycler (Bio-Rad) following the manufacturer's instructions. Quantification

434 of PCR-positive and PCR-negative droplets in each reaction, which provides absolute
435 quantification of the target transcript, was performed using the QX200 Droplet Reader (Bio-Rad).
436 This data was analyzed with QuantaSoft software (Bio-Rad) to determine the concentration of
437 each target expressed as copies per µL. Transcript copies were normalized to *tuf* mRNA (internal
438 control) and fold changes of transcripts corresponding to target genes in different mutants relative
439 to the WT parent were calculated. Statistical analysis was performed using Student's t-test with
440 GraphPad Prism version 10.0.0.
441
442 **Northern blot analysis.** Northern blotting was conducted as previously described (*13*). Briefly,
443 3 µg of isolated RNA was fractionated on 10% polyacrylamide gels containing 7% urea by
444 electrophoresis at 55 V and subsequently, transferred to a Zeta-probe membrane (Bio-Rad) using
445 a Trans-Blot SD semidry transfer apparatus (Bio-rad) at 4 mA per cm^2 with a maximum of 400
446 mA for 50 min. RNA was then UV-crosslinked to the membrane with a Spectroline UV crosslinker
447 with the "optimal crosslink" setting. 5'-Biotinylated probes were hybridized to the membrane
448 overnight at 42°C in ULTRAhyb (Ambion) hybridization buffer. Blots were developed according to
449 the BrightStar BioDetect kit protocol (Ambion), imaged with the ChemiDoc MP imager (Bio-Rad),
450 and individual band intensities were quantified using Image Lab software version 5.2.1 (Bio-Rad).
451 Signal intensities for each transcript were normalized to that of 5S rRNA, which served as a
452 loading control. Graphs of normalized abundance of each transcript for three biological replicates
453 were produced using GraphPad Prism version 10.0.0.
454
455
456 **Inductively coupled plasma-mass spectrometry (ICP-MS) analysis.** ICP-MS sample
457 preparation was based on a previous publication (*42*), with some modifications. Bacteria were
458 grown in BHI broth at 37°C with 5% CO_2 to OD_{620} = 0.2. Five mL of culture was centrifuged for 10
459 min in pre-chilled tubes at 12,400 x *g* at 4°C, and cell pellets were resuspended in 1.0 mL of

460 chilled BHI supplemented with 1 mM nitrilotriacetic acid (Sigma-Aldrich) (pH 7.2). Samples were
461 centrifuged for 7 min at 16,100 x *g* at 4°C, and supernatants were removed. Pellets were
462 centrifuged for an additional 3 min in the same way, and residual supernatant was removed. Cell
463 pellets were washed twice with centrifugation in the same way with 1.0 mL of chilled 10X PBS
464 (1.3M NaCl, 88mM Na_2HPO_4, 12mM NaH_2PO_4, pH 7.0) that had been treated with chelator.
465 Similar ICP-MS results were obtained when cells were washed with 1X PBS instead of 10X PBS.
466 Chelated PBS was prepared by mixing with 1% (wt/vol) Chelex-100 (BioRad), which was rotated
467 overnight at 4°C and passed through a 0.22 µm Steriflip (MilliporeSigma) filter. Before the last
468 centrifugation in PBS, samples were split into two 0.475 mL aliquots for ICP-MS analysis and
469 protein quantification. After removal of supernatants, pellets for ICP-MS were dried for 15 h at low
470 heat in an evaporative centrifuge and stored at -80°C until being processed for ICP-MS analysis.
471 Pellets for protein determination were suspended in in 100 µL of lysis buffer (1% (wt/vol) SDS
472 [Sigma], 0.1% w/v Triton X-100 [Mallinckrodt]) and stored at -80°C. Protein amount was
473 determined by using the DC protein assay (BioRad). For ICP-MS analysis, dried samples were
474 resuspended in 400 µL of 30% trace metal grade HNO_3 (Sigma). Samples and a 30% HNO_3 blank
475 were heated at 95° C for 10 min with shaking at 500 rpm. Samples were then diluted 100-fold to
476 a final volume of 3.0 mL with 2.5% HNO_3 containing the Pure Plus Internal Standard Mix (100
477 ppb, PerkinElmer). Samples were analyzed using an Agilent 8800 QQQ ICP-MS operating with
478 hydrogen (^{55}Mn detection) or helium (^{66}Zn detection) as collision gases to remove possible
479 interferences. ^{45}Sc or ^{72}Ge were used as internal references. Zn^{2+} and Mn^{2+} amounts were
480 calculated from standard curves made with Pure Plus Multi-Element Calibration Standard 3 (0.5-
481 100ppb, PerkinElmer). Metals amounts detected in the 30% HNO_3 blank were subtracted from all
482 samples. Metal amounts in samples were normalized relative to total protein amounts in the
483 matched samples.
484

485 **Mouse models of infection:** All procedures were approved in advance by UTHealth Animal
486 Welfare Committee and carried out as previously described (*41*). Male ICR mice (21-24 g; Envigo)
487 were anaesthetized by inhaling 4 to 5 % isoflurane. A total of 8 mice were intranasally inoculated
488 with 10^7 CFU of a specific *S. pneumoniae* strain suspended in 50 μL of 1 X PBS prepared from
489 cultures grown in BHI broth at 37°C in an atmosphere of 5% CO_2 to $OD_{620} \approx 0.1$. Mice were
490 monitored visually at 4 to 8 h intervals, and isoflurane-anesthetized moribund mice were
491 euthanized by cardiac puncture-induced exsanguination followed by cervical dislocation. Kaplan-
492 Meir survival curves and log-rank tests were generated using GraphPad Prism 10.0.0 software.
493

494 **SUPPLEMENTAL MATERIALS**

495 Supplemental Materials are available for this article.
496

497 **ACKNOWLEDGEMENTS**

498 This work was supported by NIGMS grant T32GM131994 (to M.O.), NIGMS grant R35GM118157
499 (to D.P.G.), NIGMS grant R35GM131767 (to M.E.W.), McGovern Medical Startup funds, and
500 NIAID grant R21AI171771 (to N.R.D.).
501

502 **REFERENCES**

503 1. D. G. Mediati, S. Wu, W. Wu, J. J. Tree, Networks of Resistance: Small RNA Control of
504 Antibiotic Resistance. *Trends Genet* **37**, 35-45 (2021).
505 2. R. Ghandour, K. Papenfort, Small regulatory RNAs in *Vibrio cholerae*. *Microlife* **4**, uqad030
506 (2023).
507 3. K. Papenfort, S. Melamed, Small RNAs, Large Networks: Posttranscriptional Regulons in
508 Gram-Negative Bacteria. *Annual Review of Microbiology*, (2023).
509 4. J. Hor, G. Matera, J. Vogel, S. Gottesman, G. Storz, Trans-Acting Small RNAs and Their
510 Effects on Gene Expression in *Escherichia coli* and *Salmonella enterica*. *EcoSal Plus* **9**,
511 (2020).
512 5. C. Pourciau, Y. J. Lai, M. Gorelik, P. Babitzke, T. Romeo, Diverse Mechanisms and Circuitry
513 for Global Regulation by the RNA-Binding Protein CsrA. *Frontiers in Microbiology* **11**,
514 601352 (2020).
515 6. M. G. Jorgensen, J. S. Pettersen, B. H. Kallipolitis, sRNA-mediated control in bacteria: An
516 increasing diversity of regulatory mechanisms. *Biochim Biophys Acta Gene Regul Mech*
517 **1863**, 194504 (2020).

7. L. Bossi, N. Figueroa-Bossi, P. Bouloc, M. Boudvillain, Regulatory interplay between small RNAs and transcription termination factor Rho. *Biochim Biophys Acta Gene Regul Mech* **1863**, 194546 (2020).
8. F. Ponath, J. Hor, J. Vogel, An overview of gene regulation in bacteria by small RNAs derived from mRNA 3' ends. *FEMS Microbiology Reviews* **46**, (2022).
9. G. B. D. L. R. I. Collaborators, Estimates of the global, regional, and national morbidity, mortality, and aetiologies of lower respiratory infections in 195 countries, 1990-2016: a systematic analysis for the Global Burden of Disease Study 2016. *Lancet Infect Dis* **18**, 1191-1210 (2018).
10. P. Acebo, A. J. Martin-Galiano, S. Navarro, A. Zaballos, M. Amblar, Identification of 88 regulatory small RNAs in the TIGR4 strain of the human pathogen *Streptococcus pneumoniae*. *RNA* **18**, 530-546 (2012).
11. R. Kumar *et al.*, Identification of novel non-coding small RNAs from *Streptococcus pneumoniae* TIGR4 using high-resolution genome tiling arrays. *BMC Genomics* **11**, 350 (2010).
12. B. Mann *et al.*, Control of virulence by small RNAs in *Streptococcus pneumoniae*. *PLoS Pathogens* **8**, e1002788 (2012).
13. D. Sinha *et al.*, Redefining the sRNA Transcriptome in *Streptococcus pneumoniae* Serotype 2 Strain D39. *Journal of Bacteriology*, (2019).
14. J. Slager, R. Aprianto, J. W. Veening, Deep genome annotation of the opportunistic human pathogen *Streptococcus pneumoniae* D39. *Nucleic Acids Research* **46**, 9971-9989 (2018).
15. H. C. Tsui *et al.*, Identification and characterization of noncoding small RNAs in *Streptococcus pneumoniae* serotype 2 strain D39. *Journal of Bacteriology* **192**, 264-279 (2010).
16. A. Halfmann, M. Kovacs, R. Hakenbeck, R. Bruckner, Identification of the genes directly controlled by the response regulator CiaR in *Streptococcus pneumoniae*: five out of 15 promoters drive expression of small non-coding RNAs. *Molecular Microbiology* **66**, 110-126 (2007).
17. K. Hentrich *et al.*, *Streptococcus pneumoniae* Senses a Human-like Sialic Acid Profile via the Response Regulator CiaR. *Cell Host Microbe* **20**, 307-317 (2016).
18. P. D. Rogers *et al.*, Gene expression profiling of the response of *Streptococcus pneumoniae* to penicillin. *J Antimicrob Chemother* **59**, 616-626 (2007).
19. A. Schnorpfeil *et al.*, Target evaluation of the non-coding csRNAs reveals a link of the two-component regulatory system CiaRH to competence control in *Streptococcus pneumoniae* R6. *Molecular Microbiology* **89**, 334-349 (2013).
20. F. E. Jacobsen, K. M. Kazmierczak, J. P. Lisher, M. E. Winkler, D. P. Giedroc, Interplay between manganese and zinc homeostasis in the human pathogen *Streptococcus pneumoniae*. *Metallomics* **3**, 38-41 (2011).
21. J. E. Martin, J. P. Lisher, M. E. Winkler, D. P. Giedroc, Perturbation of manganese metabolism disrupts cell division in *Streptococcus pneumoniae*. *Molecular Microbiology* **104**, 334-348 (2017).
22. B. A. Eijkelkamp *et al.*, Extracellular zinc competitively inhibits manganese uptake and compromises oxidative stress management in *Streptococcus pneumoniae*. *PloS One* **9**, e89427 (2014).
23. A. L. McFarland, N. Bhattarai, M. Joseph, M. E. Winkler, J. E. Martin, Cellular Mn/Zn Ratio Influences Phosphoglucomutase Activity and Capsule Production in *Streptococcus pneumoniae* D39. *Journal of Bacteriology* **203**, e0060220 (2021).
24. C. A. McDevitt *et al.*, A molecular mechanism for bacterial susceptibility to zinc. *PLoS pathogens* **7**, e1002357 (2011).

25. J. E. Martin *et al.*, The zinc efflux activator SczA protects *Streptococcus pneumoniae* serotype 2 D39 from intracellular zinc toxicity. *Molecular Microbiology* **104**, 636-651 (2017).
26. A. D. Ogunniyi *et al.*, Central role of manganese in regulation of stress responses, physiology, and metabolism in *Streptococcus pneumoniae*. *Journal of Bacteriology* **192**, 4489-4497 (2010).
27. J. W. Rosch, G. Gao, G. Ridout, Y. D. Wang, E. I. Tuomanen, Role of the manganese efflux system *mntE* for signalling and pathogenesis in *Streptococcus pneumoniae*. *Molecular Microbiology* **72**, 12-25 (2009).
28. J. E. Martin *et al.*, A Mn-sensing riboswitch activates expression of a Mn^{2+}/Ca^{2+} ATPase transporter in Streptococcus. *Nucleic Acids Research* **47**, 6885-6899 (2019).
29. A. Dintilhac, G. Alloing, C. Granadel, J. P. Claverys, Competence and virulence of *Streptococcus pneumoniae*: Adc and PsaA mutants exhibit a requirement for Zn and Mn resulting from inactivation of putative ABC metal permeases. *Molecular Microbiology* **25**, 727-739 (1997).
30. R. Novak, J. S. Braun, E. Charpentier, E. Tuomanen, Penicillin tolerance genes of *Streptococcus pneumoniae*: the ABC-type manganese permease complex Psa. *Molecular Microbiology* **29**, 1285-1296 (1998).
31. N. S. Jakubovics, A. W. Smith, H. F. Jenkinson, Expression of the virulence-related Sca (Mn^{2+}) permease in *Streptococcus gordonii* is regulated by a diphtheria toxin metallorepressor-like protein ScaR. *Molecular Microbiology* **38**, 140-153 (2000).
32. J. W. Johnston, D. E. Briles, L. E. Myers, S. K. Hollingshead, Mn^{2+}-dependent regulation of multiple genes in *Streptococcus pneumoniae* through PsaR and the resultant impact on virulence. *Infection and Immunity* **74**, 1171-1180 (2006).
33. C. L. Ventura, R. T. Cartee, W. T. Forsee, J. Yother, Control of capsular polysaccharide chain length by UDP-sugar substrate concentrations in *Streptococcus pneumoniae*. *Molecular Microbiology* **61**, 723-733 (2006).
34. M. B. Ayoola *et al.*, Polyamine Synthesis Effects Capsule Expression by Reduction of Precursors in *Streptococcus pneumoniae*. *Frontiers in Microbiology* **10**, 1996 (2019).
35. S. Ramos-Montanez *et al.*, Polymorphism and regulation of the *spxB* (pyruvate oxidase) virulence factor gene by a CBS-HotDog domain protein (SpxR) in serotype 2 *Streptococcus pneumoniae*. *Molecular Microbiology* **67**, 729-746 (2008).
36. K. E. Bruce, B. E. Rued, H. T. Tsui, M. E. Winkler, The Opp (AmiACDEF) Oligopeptide Transporter Mediates Resistance of Serotype 2 *Streptococcus pneumoniae* D39 to Killing by Chemokine CXCL10 and Other Antimicrobial Peptides. *Journal of Bacteriology* **200**, (2018).
37. K. M. Kazmierczak, K. J. Wayne, A. Rechtsteiner, M. E. Winkler, Roles of rel_{Spn} in stringent response, global regulation and virulence of serotype 2 *Streptococcus pneumoniae* D39. *Molecular Microbiology* **72**, 590-611 (2009).
38. B. Langmead, S. L. Salzberg, Fast gapped-read alignment with Bowtie 2. *Nature Methods* **9**, 357-359 (2012).
39. S. Anders, P. T. Pyl, W. Huber, HTSeq--a Python framework to work with high-throughput sequencing data. *Bioinformatics* **31**, 166-169 (2015).
40. M. I. Love, W. Huber, S. Anders, Moderated estimation of fold change and dispersion for RNA-seq data with DESeq2. *Genome Biol* **15**, 550 (2014).
41. D. Sinha, J. P. Frick, K. Clemons, M. E. Winkler, N. R. De Lay, Pivotal Roles for Ribonucleases in *Streptococcus pneumoniae* Pathogenesis. *mBio*, e0238521 (2021).
42. Y. Fu *et al.*, A new structural paradigm in copper resistance in *Streptococcus pneumoniae*. *Nat Chem Biol* **9**, 177-183 (2013).

619 **FIGURES**

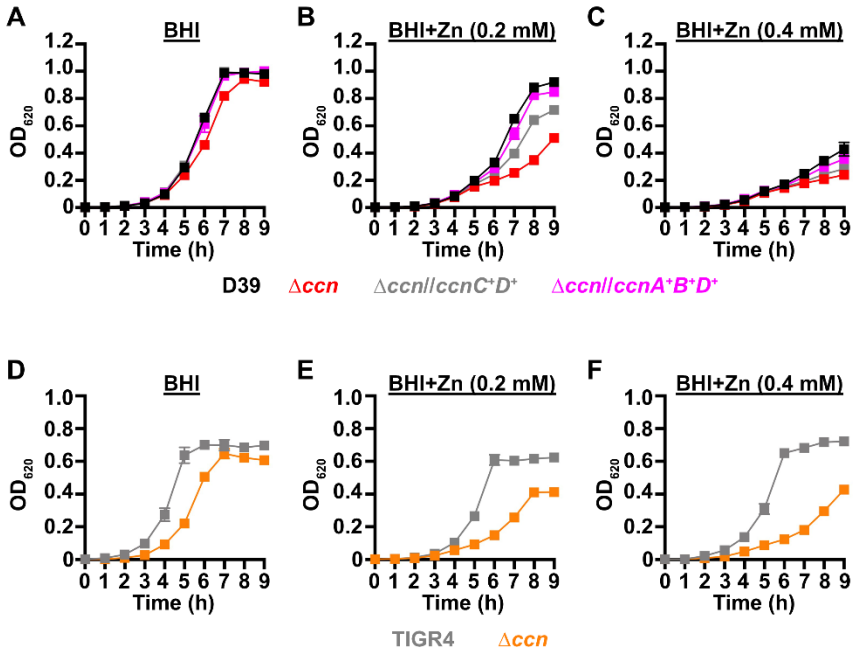

620

621 **Figure 1:** Growth phenotypes of *S. pneumoniae* strains harboring deletion of the *ccn* genes.
622 Growth characteristics at 37°C under an atmosphere of 5% CO_2 in BHI broth alone (A, D) or with
623 0.2 mM (B, E) or 0.4 mM (C,F) $ZnSO_4$ of following strains: (A, B, C) IU781 (D39), NRD10176
624 (Δ*ccn*), NRD10396 (Δ*ccn//ccnA*$^+$*B*$^+$*D*$^+$), and NRD10397 (Δ*ccn//ccnC*$^+$*D*$^+$); (D, E, F) NRD10220
625 (TIGR4) and NRD10266 (Δ*ccn*). Each point on the graph represents the mean OD_{620} value from
626 three independent cultures. Error bars, which in some cases are too small to observe in the graph,
627 represent the standard deviation (SD).

628

629

630

631

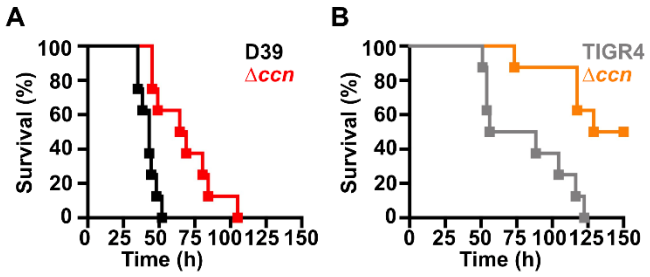

632

633 **Figure 2:** Virulence phenotypes of *S. pneumoniae* strains harboring deletion of the *ccn* genes.
634 Survival curve of ICR outbred mice after infection with ~10^7 CFU in a 50 μL inoculum of the
635 following *S. pneumoniae* strains: (A) IU1781 (D39) and NRD10176 (Δ*ccn*); (C) NRD10220
636 (TIGR4) and NRD10266 (Δ*ccn*). Eight mice were infected per strain. Disease progression of
637 animals was monitored, the time at which animals reached a moribund state was recorded, and
638 these mice were subsequently euthanized as described in Materials and Methods. A survival
639 curve was generated from this data and analyzed by Kaplan-Meier statistics and log rank test to
640 determine P-values.

641

642

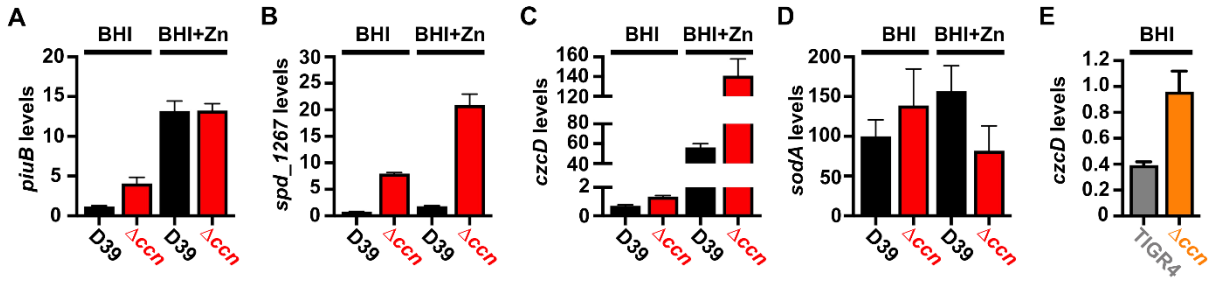

643

644 **Figure 3:** Loss of the *ccn* genes perturbs the expression of Zn and Mn stress associated genes
645 in *S. pneumoniae*. Abundance of *piuB* (A), *spd_1267* (B), *czcD* (C, E), and *sodA* (D) mRNAs was
646 determined by RT-ddPCR (A, B, and C) or northern blot analyses (D) as described in Materials
647 and Methods for strain IU1781 (D39) and derived Δ*ccnABCDE* mutant strain (NRD10176; Δ*ccn*)
648 grown to exponential phase (OD_{620} of ~0.2) in BHI broth alone (BHI) or supplemented with 0.2

649 mM Zn (BHI+Zn) at 37°C under an atmosphere of 5% CO_2. (E) Expression of *czcD* was
650 determined by RT-ddPCR analyses for NRD10220 (TIGR4) and derived Δ*ccnABCDE* mutant
651 strain NRD10266 (Δ*ccn*) grown to exponential phase in BHI Broth at 37°C under an atmosphere
652 of 5% CO_2. Transcript levels were normalized to *tuf* (A, B, C, and E) or 5S rRNA (D). Values
653 represent the mean of three independent cultures and error bars indicate SEM.
654
655

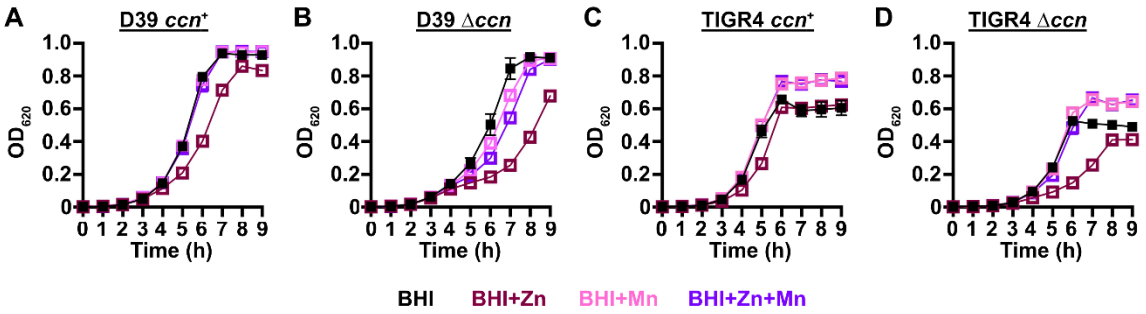

656
657 **Figure 4:** Mn supplementation eliminates the Zn dependent growth inhibition of *S. pneumoniae*
658 Δ*ccnABCDE* mutant. Growth characteristics at 37°C under an atmosphere of 5% CO_2 in BHI broth
659 alone (BHI) or with 0.2 mM $ZnSO_4$ (BHI+Zn), 0.2 mM $MnCl_2$ (BHI+Mn), or 0.2 mM $ZnSO_4$ and
660 $MnCl_2$ (BHI+Zn+Mn) of strains (A) IU1781 (D39 *ccn*⁺), (B) NRD10176 (D39 Δ*ccn*), (C), NRD10220
661 (TIGR4 *ccn*⁺), and (D) NRD10266 (TIGR4 Δ*ccn*). Each point on the graph represents the mean
662 OD_{620} value from three independent cultures. Error bars, which in some cases are too small to
663 observe in the graph, represent the standard deviation (SD).
664
665
666
667
668
669

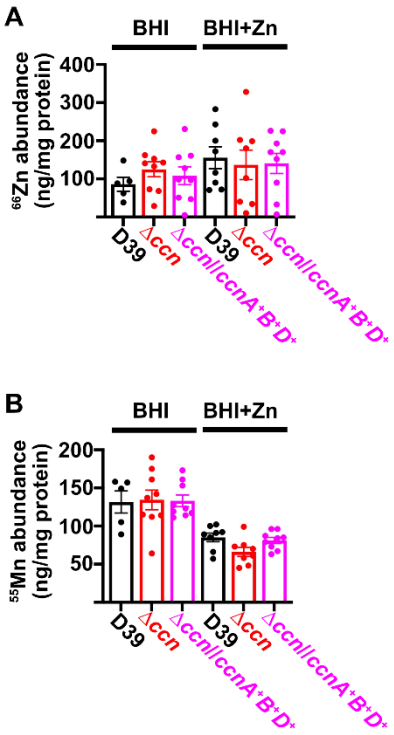

Figure 5: Deletion of the *ccn* genes reduces total cell associated Mn, but not Zn levels. Total cell associated Zn (A) and Mn (B) was measured from cells harvested from cultures of IU781 (D39), NRD10176 (Δ*ccn*), and NRD10396 (Δ*ccn//ccnA*$^+$*B*$^+$*D*$^+$) grown to exponential growth phase (OD_{620} of ~0.2) in BHI broth alone (BHI) or with 0.2 mM ZnS04 (BHI+Zn) by ICP-MS and normalized to protein amounts. Results represent the mean of 5 to 9 replicates with values from each replicate shown as a point. Error bars indicate SEM.

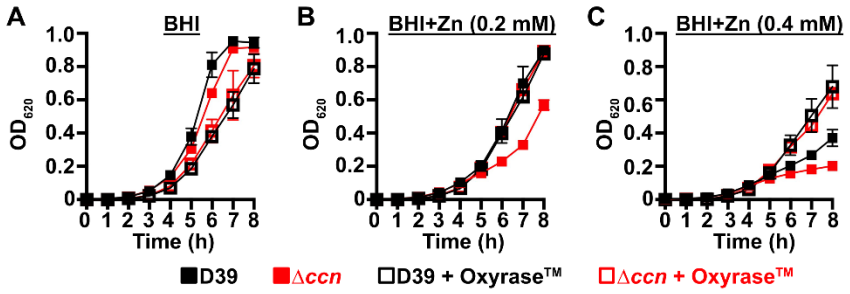

Figure 6: Depletion of O_2 abolishes the Zn hypersensitivity of the *S. pneumoniae* Δ*ccnABCDE* mutant. Growth characteristics at 37°C under an atmosphere of 5% CO_2 in BHI broth alone (A) or with 0.2 mM (B) or 0.4 mM (C) $ZnSO_4$ of IU781 (D39) and NRD10176 (Δ*ccn*) in the absence or presence of 10% (volume/volume) Oxyrase™. Each point on the graph represents the mean OD_{620} value from three independent cultures. Error bars, which in some cases are too small to observe in the graph, represent the standard deviation (SD).

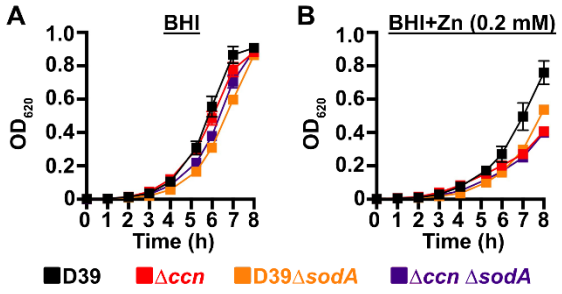

Figure 7: A *S. pneumoniae* Δ*sodA* mutant phenocopies the Zn hypersensitivity of a Δ*ccnABCDE* mutant strain. Growth characteristics at 37°C under an atmosphere of 5% CO_2 in BHI broth alone (A) or with 0.2 mM $ZnSO_4$ (B) of IU781 (D39), NRD10176 (Δ*ccn*), NRD10533 (D39 Δ*sodA*), and NRD10534 (Δ*ccn* Δ*sodA*). Each point on the graph represents the mean OD_{620} value from three independent cultures. Error bars, which in some cases are too small to observe in the graph, represent the standard deviation (SD).

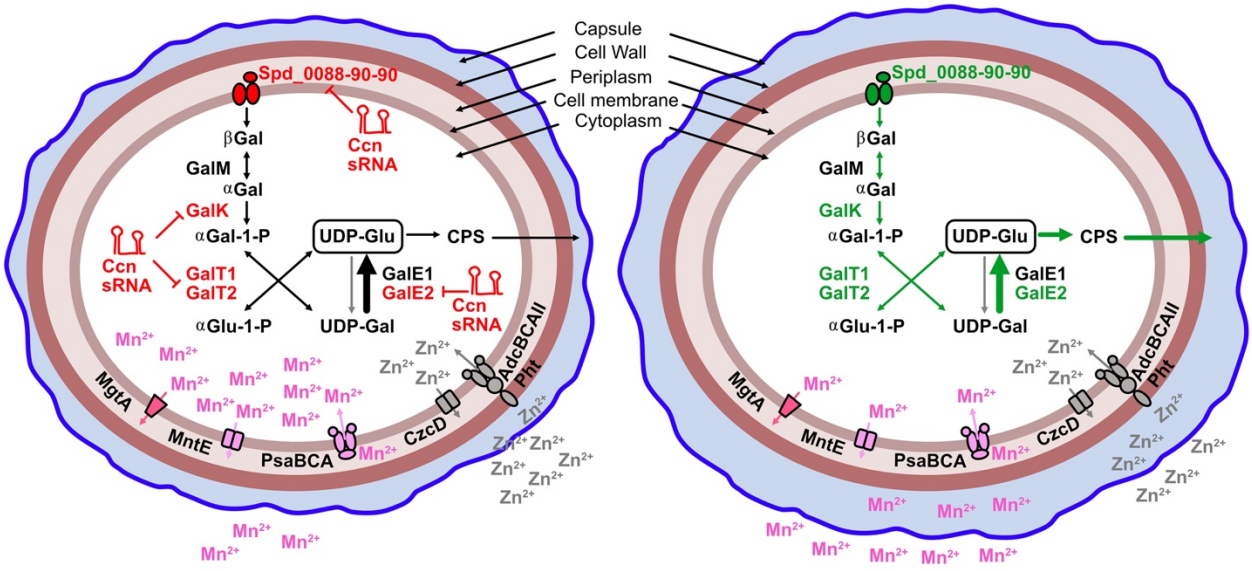

Figure 8: Model of the function of the Ccn sRNAs in regulating Mn homeostasis. The Ccn sRNAs down-regulate expression of Leloir pathway (*galK*, *galT2*, *galT1*, *galE2*) and galactose transport genes (*spd_0088*, *spd_0089*, *spd_0090*) resulting in reduced CPS synthesis and thus, a thinner capsule, which improves Mn uptake (pneumococcal cell on the left). In the absence of the Ccn sRNAs, increased expression of the Leloir pathway genes leads to increased production of capsule precursors and consequently, increased capsule thickness limiting Mn uptake (pneumococcal cell on the right). MgtA (Ca^{2+}/Mn^{2+} exporter); MntE (primary Mn^{2+} exporter); PsaBCA (only known Mn^{2+} importer); CzcD (Cd^{2+}/Zn^{2+} exporter); Pht (histidine triad proteins that bind Zn^{2+} and transfer to AdcAII); AdcBCAII (Zn^{2+} import system).